Anti-VEGF treatment improves neurological function and augments radiation response in NF2 schwannoma model

Xing Gao[a,b,1], Yingchao Zhao[a,c,1], Anat O. Stemmer-Rachamimov[d], Hao Liu[a], Peigen Huang[a], ShanMin Chin[a], Martin K. Selig[d], Scott R. Plotkin[e], Rakesh K. Jain[a], and Lei Xu[a,2]

[a]Department of Radiation Oncology, Massachusetts General Hospital and Harvard Medical School, Boston, MA 02114; [b]Department of Oral and Maxillofacial Surgery, Xiangya Hospital, Central South University, Changsha, Hunan 410008, China; [c]Cancer Center, Union Hospital, Tongji Medical College, Huazhong University of Science and Technology, Wuhan, Hubei 430023, China; [d]Molecular Pathology Division, Massachusetts General Hospital and Harvard Medical School, Boston, MA 02114; and [e]Department of Neurology and Cancer Center, Massachusetts General Hospital and Harvard Medical School, Boston, MA 02114

Hearing loss is the main limitation of radiation therapy for vestibular schwannoma (VS), and identifying treatment options that minimize hearing loss are urgently needed. Treatment with bevacizumab is associated with tumor control and hearing improvement in neurofibromatosis type 2 (NF2) patients; however, its effect is not durable and its mechanism of action on nerve function is unknown. We modeled the effect anti-VEGF therapy on neurological function in the sciatic nerve model and found that it improves neurological function by alleviating tumor edema, which may further improve results by decreasing muscle atrophy and increasing nerve regeneration. Using a cranial window model, we showed that anti-VEGF treatment may achieve these effects via normalizing the tumor vasculature, improving vessel perfusion, and delivery of oxygenation. It is known that oxygen is a potent radiosensitizer; therefore, we further demonstrated that combining anti-VEGF with radiation therapy can achieve a better tumor control and help lower the radiation dose and, thus, minimize radiation-related neurological toxicity. Our results provide compelling rationale for testing combined therapy in human VS.

NF2 schwannoma model | anti-VEGF | neurological function | radiation

Neurofibromatosis type 2 (NF2) is a dominantly inherited genetic condition with a birth prevalence of 1 in 25,000 (1). Bilateral vestibular schwannomas (VS), which are benign tumors composed of neoplastic Schwann cells that arise from the eighth cranial nerve, are the hallmark of NF2 (2). Standard approaches for treatment of growing VS include surgical removal and radiation therapy (RT). Hearing loss is the main limitation of radiation therapy for VS. For patients with sporadic VS who do not have NF2, RT is associated with long-term tumor control rates exceeding 95%. However, hearing preservation rates after radiation range from 50% to 80% (3, 4). Outcomes after radiation for patients with NF2 are inferior to those for sporadic patients, with short-term local tumor control rates approximately 80–85% and hearing preservation rates <50% (3). Thus, the identification of a novel adjunct therapy to enhance radiosensitivity while minimizing toxicity-related hearing loss in VS is urgently needed.

Vascular endothelial growth factor (VEGF) and its receptors (VEGFRs) are expressed in VS, and its expression level positively correlates with schwannoma growth rate (5–7). In a retrospective review of 31 NF2 patients, treatment with bevacizumab, a humanized monoclonal antibody that specifically neutralizes VEGF-A, was associated with a reduction in the volume of most growing VS. More importantly, bevacizumab treatment improved hearing in 57% patients (7). Despite this progress, a number of challenges remain (8). First, not all NF2 patients respond to bevacizumab; second, the hearing response is not durable in all patients; and third, some patients are unable to tolerate long-term bevacizumab treatment. Studies to understand the mechanisms of anti-VEGF therapy-induced tumor growth inhibition and

hearing improvement in schwannomas are urgently needed to optimize this therapy.

In our study, first, we used the sciatic nerve model to characterize the effect and mechanisms of anti-VEGF treatment on neurological function. We revealed that anti-VEGF treatment alleviates tumor edema, which may further result in decreasing muscle atrophy and increasing nerve regeneration and, thus, improves neurological function. Second, we used the intracranial window model to monitor in real time the effect of anti-VEGF treatment on tumor vasculature. We showed that anti-VEGF treatment transiently normalizes the tumor vasculature, leading to improved perfusion and oxygen delivery. Using intravital microscopy imaging technique, we further defined the timing of this transient effect, termed the "normalization window," in schwannoma models. Because oxygen is a potent radiosensitizer, finally, we showed that radiation therapy applied during the normalization window is most effective, and combined anti-VEGF and radiation therapy is superior to each monotherapy. Anti-VEGF and radiation combination therapy may thus help reduce the dose of each therapy and minimize treatment-associated adverse effect in NF2 patients.

Significance

In patients with progressive vestibular schwannoma (VS), radiotherapy is associated with risk of debilitating hearing loss. There is an urgent need to identify an adjunct therapy that, by enhancing the efficacy of radiation, can help lower the radiation dose and improve hearing preservation. Bevacizumab improved hearing in neurofibromatosis type 2 patients; however, its effect is not durable and its mechanism of action on nerve function is unknown. Our study provides (*i*) insight into how anti-VEGF treatment improves neurological function, and (*ii*) critical data that combined anti-VEGF treatment can enhance the efficacy of radiation therapy and help lower its dose. Our findings support clinical evaluation of combined anti-VEGF and radiation therapy in patients with VS.

Results

Anti-VEGF Treatment Improves Neurological Function. First, we studied the effect of anti-VEGF treatment on neurological function in mice. To faithfully represent the effect of bevacizumab, we used an antibody (B20.4.4; Genentech) that neutralizes both human (tumor) and mouse (host) VEGF in our animal studies. We performed rotarod test to evaluate neurological function; starting as early as 6 h after the first B20 treatment, rotarod duration increased and became significantly improved after 24 h (Fig. S1). To examine the effect of different treatments on neurological function, mice bearing same-sized tumors were treated with control IgG, radiation (5 Gy), B20, or combined B20 and radiation. Before treatment, no significant differences were noted from the rotarod test in mice among different groups. After B20 treatments, mice showed significantly improved rotarod performance compared with mice in control and RT groups (Fig. 1A). In the following studies, we further examined three aspects that anti-VEGF treatment may affect and thus contribute to this improved neurological function: (*i*) tissue edema, (*ii*) muscle atrophy, and (*iii*) nerve damage/regeneration.

Anti-VEGF Treatment Reduces Tumor Edema. Tissue edema may increase interstitial fluid pressure, which can compress nerves and muscles to cause weakness or stiffness (9, 10). In mice and patients with glioblastoma (GBM), anti-VEGF therapy has been shown to alleviate tumor edema by reducing vascular permeability within 6 h and 24 h, respectively (10–12). Our observation that rotarod performance improved after 6 h of anti-VEGF treatment indicates a change in schwannoma edema. Indeed, we found that the degree of tumor edema was significantly inversely correlated with rotarod duration (Fig. 1B), supporting that edema may impair neurological function. Furthermore, B20 treatment alone, and in combination with RT (5 Gy) significantly decreased edema (Fig. 1C).
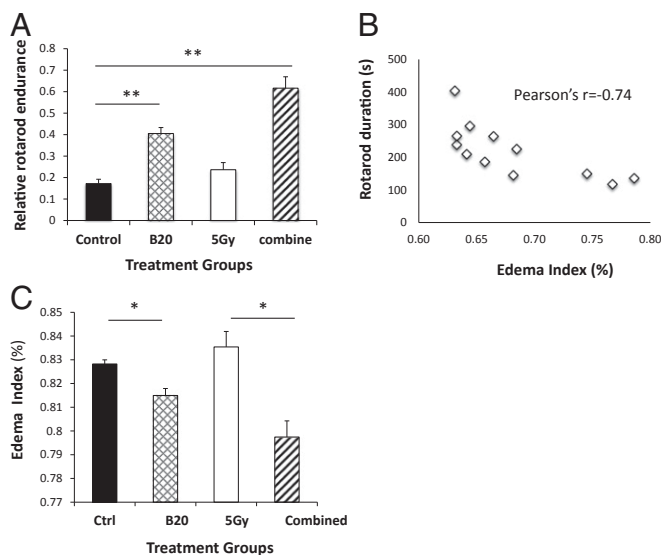

Fig. 1. Anti-VEGF treatment improves rotarod performance and decreases $Nf2^{-/-}$ tumor tissue edema. (A) Rotarod test was carried out in mice bearing size-matched tumors, followed by tumor collection to evaluate edema (B and C). The average time to fall from the rotating cylinder was normalized to the value from each mouse on the first day and presented as relative rotarod endurance. (B) Edema index significantly inversely correlates with rotarod duration. Pearson product moment correlation coefficient $r = -0.7416$, $P = 0.006$. (C) B20 treatment, as monotherapy as well as in combination with radiation therapy (5 Gy), significantly decreased tumor edema. Representative of at least three independent experiments ($n = 8$), data presented are mean ± SEM. *$P < 0.01$, **$P < 0.005$.

Anti-VEGF Treatment Decreases Muscle Atrophy. Muscle atrophy is a common consequence of peripheral nerve lesions such as tumors. We assessed the effect of anti-VEGF treatment on muscle atrophy by measuring: (*i*) the cross-sectional area of single muscle fibers and (*ii*) the distribution of muscle fiber size. From both legs, we collected the gastrocnemius muscle, which is distal to the sciatic nerve tumor implantation site and is not directly damaged by tumor growth. Nontumor bearing mice had large and uniform skeletal muscle fibers, with the average muscle fiber area of $2,123.4 \pm 127.8$ μm^2, and the majority of gastrocnemius muscle fibers had an area in the range of $1,000$–$1,400$ μm^2. None of the treatments affected muscle fiber size and distribution in the nontumor-bearing leg. In tumor-bearing leg from control and radiated mice, significant muscle atrophy was noted, demonstrating significantly decreased muscle fiber area, and the majority of gastrocnemius muscle fiber area is in the range of 400–800 μm^2. B20 treatment significantly increased average muscle fiber area and shifted the distribution peak toward the normal range in the tumor-bearing leg (Fig. 2).

Anti-VEGF Treatment Enhances Nerve Regeneration. It is known that muscle atrophy occurs after complete denervation—when the nerve supply to a muscle is interrupted, the muscle no longer receives signals or stimuli from the nervous system (13). Therefore, we next evaluated the effect of anti-VEGF therapy on nerve damage and regeneration. The tibial nerve in the control group presented with edema, and B20 treatment significantly decreased nerve edema (Fig. 3A). Under electron microscopy (EM), there is a marked deficit or abnormal appearance of axons in the cross-sections of the tibial nerve from control and radiated mice, demonstrating scattered degenerating axons, macrophage infiltration, and empty Schwann cell stacks, indicating loss of myelinated and unmyelinated axons. In contrast, sections from anti-VEGF–treated animals showed regenerating clusters, thinly myelinated axons, which are consistent with regeneration and remyelination (Fig. 3B). We examined the expression of several molecules that are known to mediate nerve regeneration; there is a trend toward up-regulation of these genes by B20 treatment, but only CXCL1 [chemokine (C-X-C motif) ligand 1] was significantly induced more than twofold (Fig. 3C).

Anti-VEGF Treatment Normalizes Vasculature. Abnormal vascular perfusion has been associated with muscular atrophy and nerve damage (14–17). Next, in the cranial window model, we used intravital microscopy imaging to observe vascular changes in real time. We found that control tumors have dilated and tortuous vessels, and B20 treatment makes tumor vessels less tortuous and smaller in diameter (Fig. 4A). Quantification of the image confirmed that B20-treated mice have decreased vessel diameter, vessel number, surface area, and length compared with that of the control group. These changes started 2 days after B20 treatment and continued to day 5, but were less pronounced on day 8, indicating the vessel normalization phenomenon is transient, and the normalization window is between day 2 and day 5 (Fig. 4 B–E). This vascular normalization effect was similarly observed in HEI-193 intracranial model (Fig. S2), and the decreased microvessel density (MVD) was confirmed in the sciatic nerve model (Fig. 5 A and B).

Tumor vessels have fewer pericytes, which support the endothelial surface of blood vessel walls, and this structural abnormality lead to abnormal vessel perfusion (18, 19). We found that anti-VEGF treatment increased the fraction of pericyte-covered vessels, indicating the schwannoma vasculature is structurally close to normal vessels (Fig. 5). Next, to determine whether structural normalization of tumor vessels translates into improved functional perfusion, we measured the fraction of perfused vessels by injecting FITC-lectin i.v. to identify perfused tumor vessels and by staining for CD31 to detect the total number of blood vessels. In concert with the vessel morphological and structural changes, B20 treatment increased the percentage of perfused vessels more than threefold (Fig. 5C). As a result of improved vessel perfusion, we
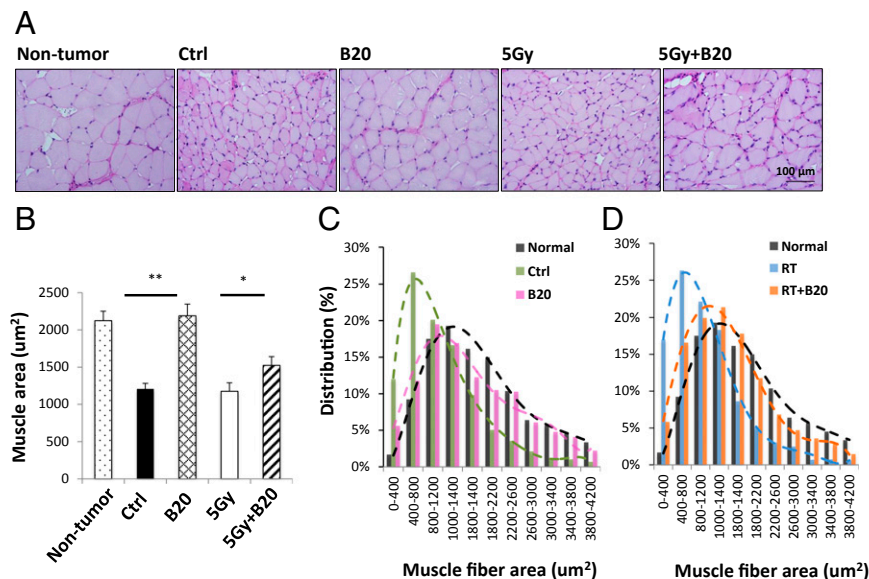
MEDICAL SCIENCES

Fig. 2. Anti-VEGF treatment decreases muscle atrophy. (*A*) Representative images of periodic acid Schiff's (PAS) staining. When tumors reached 1 cm in diameter, mice were killed and gastrocnemius muscles from both normal and tumor-bearing legs were collected for histological analysis. (Scale bar: 100 μm.) (*B*) Single fiber areas in 10 randomly selected microscopic fields were quantified by using ImageJ software. Data presented are mean ± SD. *$P < 0.05$, **$P < 0.01$. Histogram of muscle fiber area distribution comparing nontumor bearing mice (black, $n = 1,088$ muscle fibers) with tumor-bearing control mice (green, $n = 1,289$ muscle fibers) and B20-treated mice (pink; $n = 930$ muscle fibers) (*C*); and nontumor bearing mice (black) with radiation (blue; $n = 1,712$ muscle fibers) and combination therapy treated mice (orange; $n = 1,249$ muscle fibers) (*D*).

found the hypoxic fraction of the viable schwannomas was significantly lower in B20-treated mice (Fig. 5*D*). Collectively, our studies show that B20 treatment improves the schwannoma vessel perfusion and alleviates tumor hypoxia, which may contribute to the improved neurological function.

Radiation Therapy Applied During the Anti-VEGF Induced Normalization Window Shows Improved Efficacy. Hypoxic cells are more resistant to radiation (20); therefore, we further hypothesized that the improved oxygenation may enhance the cytotoxic effect of RT, and when radiation is applied during the vascular normalization window, it would be most effective. Indeed, in the $Nf2^{-/-}$ intracranial model, when radiation was applied during the normalization window (2 d after B20 treatment), it significantly extended survival and inhibited tumor growth over B20 or radiation monotherapy. When radiation was applied outside the normalization window (2 d before B20 treatment), the combined therapy had no additive effect compared with each monotherapy (Fig. 6 *A* and *B*). This effect was confirmed in our sciatic nerve model—combination therapy induced an 8-d tumor growth delay, more than monotherapy with B20 (4 d) or RT (3 d; Fig. 6 *C* and *D*). The same effect of B20-enhanced radiation efficacy was observed in HEI-193 intracranial and sciatic nerve models (Fig. S3). These studies support our hypothesis that radiation applied during the vascular normalization window induced by anti-VEGF treatment is most effective.

To evaluate whether B20 enhances RT efficacy via direct antitumor effects, we examined the expression and function of VEGF-A in schwannoma cell lines. Our study showed that although both $Nf2^{-/-}$ and HEI-193 cells express VEGF-A and its receptors R1 and R2, B20 treatment does not directly affect: (*i*) tumor cell proliferation, (*ii*) DNA damage, (*iii*) radiosensitivity, or (*iv*) angiogenic gene expression (Fig. S4). These studies suggest that B20 enhanced the efficacy of radiotherapy through the host vascular remodeling and normalization effect.

Anti-VEGF Treatment Combined with Low-Dose Radiation Is as Effective as High-Dose Radiation. To determine whether by combining anti-VEGF therapy with RT, we can lower the dose and, thus, the adverse effect of RT, we treated groups of mice with: (*i*) control, (*ii*) B20, (*iii*) 5 Gy, (*iv*) 10 Gy and (*v*) B20 + 5 Gy. In both $Nf2^{-/-}$ and HEI-193 sciatic nerve models, we found that 10-Gy radiation is significantly more effective than the 5 Gy. However, when combined with B20 treatment, 5-Gy radiation is as effective

as 10-Gy radiation in the $Nf2^{-/-}$ model (Fig. 6*E*) and significantly more effective than 10-Gy radiation in the HEI-193 model (Fig. S3*E*). These studies suggest that combining anti-VEGF treatment may help lower the radiation dose needed to control schwannoma growth and, thus, may minimize RT side effect.

Discussion

In this study, we sought to determine: (*i*) the mechanism of anti-VEGF improved neurological function, and (*ii*) whether combined anti-VEGF treatment can enhance the efficacy of radiation therapy and help lower its dose and, thus, minimize its toxic side effect on neurological function in schwannoma animal models.

Schwannomas of the cranial, spinal, and peripheral nerves originate from the nerve sheath and damage the nerve as they grow,
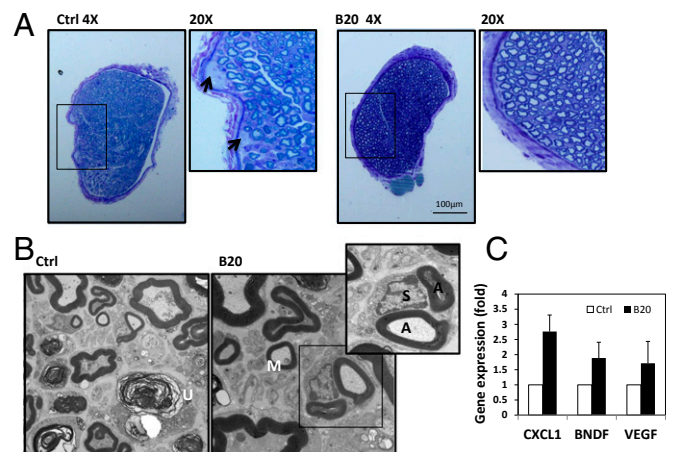

Fig. 3. Anti-VEGF treatment enhances nerve regeneration. (*A*) Representative images of toluidine blue staining. When tumor reached 1 cm in diameter, mice were killed and the tibial nerves were collected for histological analysis. Arrows are pointing to edema and focal fluid collection in the control nerve. (*B*) Representative electron microscopy images of the tibial nerve of mice bearing sciatic nerve tumors. In control group, unmyelinated axons (U) were evident, indicating degenerating axons. In B20 group, thinly myelinated axon (M, consistent with remyelination and regeneration) and regenerating clusters (a Schwann cell (S) associated with two myelinated axons (A) were evident, indicating nerve regeneration. (*C*) Quantitative RT-PCR analysis of the $Nf2^{-/-}$ sciatic nerve tumors.
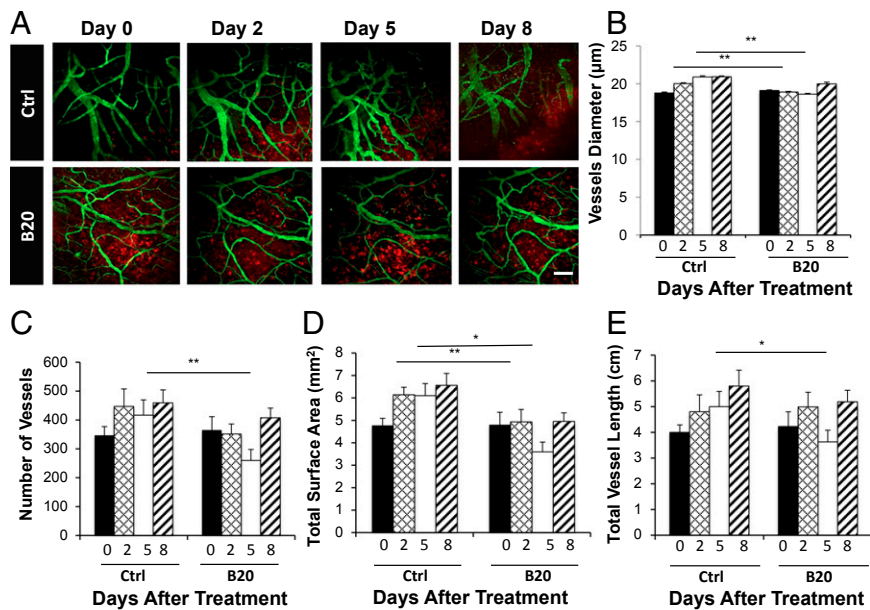
Fig. 4. Inhibition of VEGF signaling reduces number and density of schwannoma vessels. (*A*) Representative in vivo multiphoton laser scanning microscopy images of blood vessels (green) in $Nf2^{-/-}$ tumors (red) grown in the cranial window of nude mice on day 0, 2, 5, and 8 after treatment. Control, $n = 10$; B20, $n = 8$. (Scale bar: 100 μm.) Quantification of vessel diameter (*B*), total number of vessels (*C*), total vessel surface area (*D*), and total vessel length (*E*); comparison was made to the control group. Data are representative of at least three independent experiments and are presented as mean ± SD., *$P < 0.05$, **$P < 0.01$.

causing neurological dysfunction (1, 21, 22) and any treatment that could relieve these symptoms is highly desirable. Radiation therapy can further cause hearing loss by inducing local damage to mature nerve tissue, which is partly attributable to microvascular injury (23, 24). Whereas the role of VEGF on tumor angiogenesis and progression has been well characterized, the role of anti-VEGF treatment on tumor-related neuropathy remains largely unknown. We reproduced the ability of anti-VEGF treatment to improve neurological performance in the sciatic nerve xenograft model; we showed that anti-VEGF treatment potentially affects the function of nerve and muscle via reducing tissue edema, which may further decrease muscle atrophy and improve nerve regeneration. In mice, it is technically challenging to orthotopically implant schwannomas in the vestibular nerve and performs functional vestibular studies and hearing test (25). Models for the development of new treatment options in VS are lacking. Transgenic and xenograft mouse

models of VS have been previously reported in the literature (26, 27). However, none of these models replicate the intracranial location of these tumors in human disease. Recently, a novel NF2 mouse model generated through excision of the *Nf2* gene under the control of schwann cell-specific promoter element demonstrated spinal, peripheral, and cranial nerve tumors histologically identical to human schwannomas (28). This new model would permit testing of the vestibular nerve function and hearing response for VS translational studies. Although we cannot directly translate our findings from a major motor nerve to a cranial nerve, our data pave the road for further study of the molecular mechanisms of the effect of anti-VEGF treatment on neurological function.

The effect of VEGF on nerves has been studied in neurodegenerative disease (such as amyotrophic lateral sclerosis) (15), and in acute neurological disease (such as cerebral ischemia) (29, 30). In these disease models, it has been shown that the effect
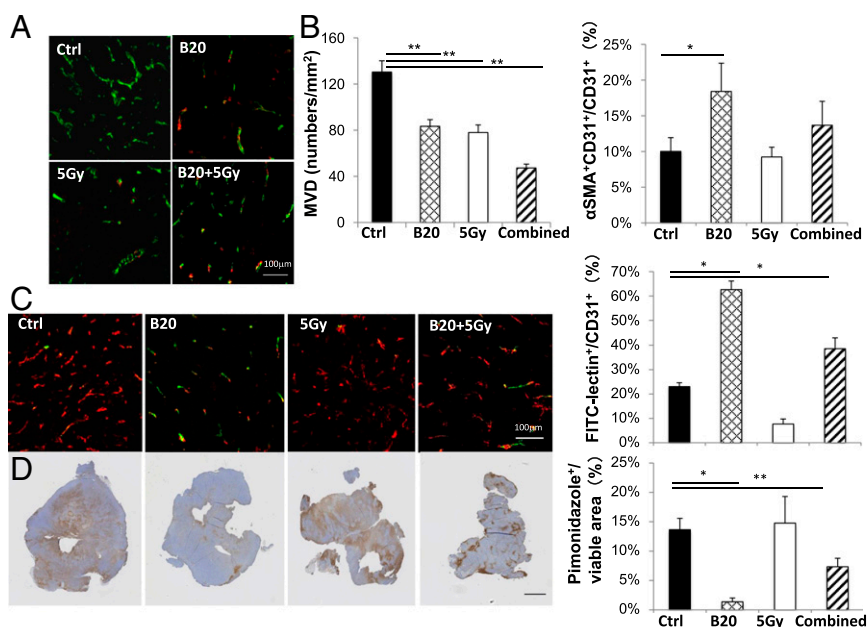

Fig. 5. Inhibition of VEGF signaling normalizes schwannoma vessel structure, increases schwannoma blood vessel perfusion, and relieves tumor hypoxia. $Nf2^{-/-}$ schwannomas were collected on day 5 after treatment. (*A*) Representative immunofluorescent staining images of CD31 (an endothelial cell marker, green) and αSMA (a pericyte marker, red). (*B*) Microvessel density (MVD) and the fraction of pericyte covered vessels (% αSMA$^+$CD31$^+$/CD31$^+$) were quantified by using ImageJ software. (*C*) Representative immunofluorescent staining and quantification of the fraction of perfused blood vessels (green, FITC-lectin) among all vessels (red, CD31). Yellow, CD31$^+$ staining of perfused vessels. (*D*) Representative immunohistochemical staining and quantification of the hypoxic fraction of the viable (nonnecrotic) tumor tissue area (pimonidazole$^+$, brown). Data presented are mean ± SD. *$P < 0.05$, **$P < 0.01$. (Scale bar: *A* and *C*, 100 μm; *D*, 1 mm.)
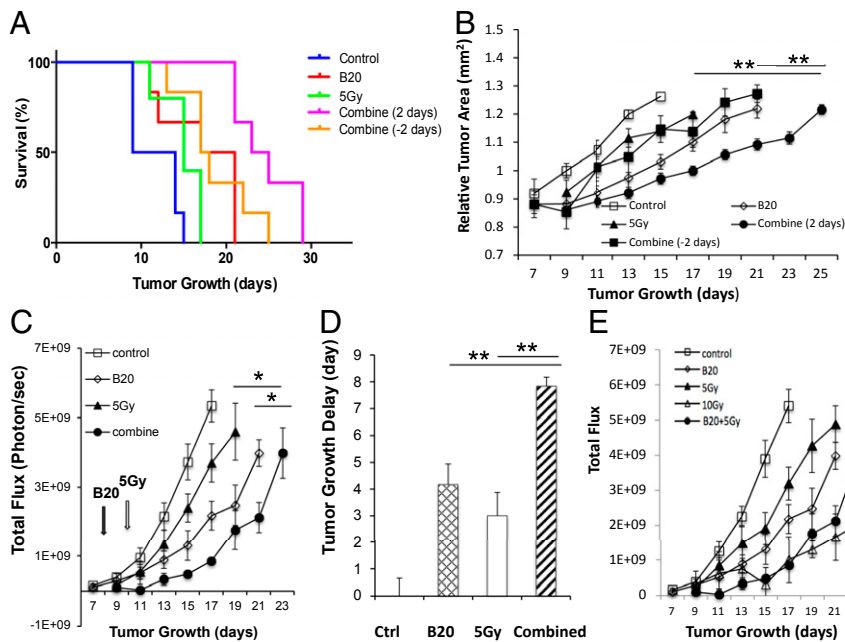
MEDICAL SCIENCES

Fig. 6. Combination therapy more effectively inhibits growth of $Nf2^{-/-}$ schwannomas. Kaplan–Meier survival curves (*A*) and tumor growth curves (*B*) of mice in $Nf2^{-/-}$ cranial window model. Tumor growth in control, B20, 5 Gy, and two different combination groups [radiation given 2 d before (combine −2 d) or after (combine 2 d) B20 treatment] were measured by OFDI ($n = 8$). **, combined (2 d) compared with B20 or radiation only groups. (*C*) Tumor growth was measured by whole body imaging (WBI, $n = 8$) in $Nf2^{-/-}$ sciatic nerve tumor. (*D*) Tumor growth delay (vs. control) was defined by the time taken for tumors to double their WBI reading. (*E*) Tumor growth in control, B20, 5 Gy, 10 Gy, and B20 combined with 5 Gy were measured by WBI. Representative of at least three independent experiments, all data presented are mean ± SEM. *$P < 0.05$, **$P < 0.01$.

of VEGF on nerve is twofold: (*i*) VEGF exerts direct neuroprotective effects on cultured neurons in vitro (15, 31, 32); and (*ii*) VEGF stimulates angiogenesis, which is thought to provide an "angiogenic niche" that improves neural perfusion and favors neuronal progenitor proliferation and differentiation in vivo (15–17, 33). In a genetic study where the hypoxia response element (HRE) of the *Vegfa* promoter is mutated, serum VEGF level decreases, resulting in decreased neural perfusion and spinal cord ischemia, ultimately leading to neuron degeneration and progressive paralysis (34). We found that anti-VEGF treatment, by normalizing schwannoma vasculature, improved tumor blood vessel perfusion and oxygen delivery and, thus, our finding is consistent with the HRE knock-out study. It has been well documented that although tumors harbor excess blood vessels, the tumor vascular network is highly abnormal, leading to aberrations in local blood flow and oxygenation that, in turn, can fuel tumor growth, invasion, and metastasis while diminishing response to cytotoxic therapies (9). It has been shown in many preclinical and clinical studies that antiangiogenic therapy prunes tumor vessels and reverts the abnormal structure and function of the remaining vasculature toward a more normal state, abrogating its deleterious effects on the tumor microenvironment (9). In GBM patients, anti-VEGF treatment-induced vascular normalization alleviated vasogenic edema (11). In our schwannoma model, whether the improved vessel perfusion and oxygenation induced by anti-VEGF treatment contributes to muscle atrophy and/or nerve regeneration directly or via reducing tumor growth and relieving edema remains to be determined.

Anti-VEGF agents were originally developed to block tumor growth by inhibiting blood vessel formation (19, 35). Bevacizumab failed to improve survival benefit as a monotherapy in a number of tumors, but conferred survival benefit in combination with chemotherapy or immunotherapy (19). A potential explanation for the success of combined therapies is that bevacizumab "normalizes" the abnormal vasculature of tumors; the effect is transient—leading to a normalization window—during which, the resulting vasculature is more normal, characterized by increased blood flow and improved delivery of concurrently administered anticancer drugs as well as oxygen (19). In our schwannoma model, the anti-VEGF–induced normalization window is between day 2 and day 5. This observation is consistent with previously published vessel dynamic changes

—preclinical GBM study showed that anti-VEGF treatment decreased vessel density in 2 days, and clinical data in recurrent GBM patients demonstrate that antiangiogenic agents induced vascular normalization within 24 hours (11, 36). Clinical studies of relative vessel size and permeability, tumor contrast enhancement, and edema-associated parameter are needed to fully elucidate the normalization effect of bevacizumab in NF2 patients.

Preclinical and clinical studies showed that vessel normalization improves the efficacy of conventional chemotherapy and radiation therapy, because both rely on adequate tumor blood flow for the delivery of drugs and radiosensitizing oxygen (19, 37). In an experimental study in mice with GBM, combining anti-VEGF therapy enhanced the efficacy of radiation therapy (36). Phase I/II trials reported promising response rates and safety results for adding bevacizumab before and concurrent to chemoradiation therapy in the preoperative treatment of locally advanced rectal cancer (38–41). However, the response rate varied, indicating the importance of a good selection of patients for this combination treatment, as well as prospectively validated biomarkers of response (39, 42–46). Our study showed that in schwannoma model, when radiation is applied during the normalization window, it is more effective than either therapy alone; providing useful information on the timing and schedule of radiation therapy relative to anti-VEGF treatment. Furthermore, we showed that combining anti-VEGF treatment helps lower the radiation dose needed for tumor control and, thus, may help relieve the toxic radiation side effect. Biomarkers of response and resistance to bevacizumab treatment are needed to improve the efficacy of this approach in patients with schwannomas.

In summary, this study demonstrated that integrating anti-VEGF with RT in schwannoma models is more effective than either therapy alone and may reduce neurological dysfunction related to tumor growth and radiation (Fig. S5). Our study provides the rationale and critical data for the clinical translation of combining anti-VEGF with radiation therapy in patients with VS.

Methods

1. Evans DG, et al. (1992) A clinical study of type 2 neurofibromatosis. *Q J Med* 84(304): 603–618.
2. Plotkin SR, Merker VL, Muzikansky A, Barker FG, 2nd, Slattery W, 3rd (2014) Natural history of vestibular schwannoma growth and hearing decline in newly diagnosed neurofibromatosis type 2 patients. *Otol Neurotol* 35(1):e50–e56.
3. Ammoun S, Hanemann CO (2011) Emerging therapeutic targets in schwannomas and other merlin-deficient tumors. *Nat Rev Neurol* 7(7):392–399.
4. Plotkin SR, et al. (2012) Bevacizumab for progressive vestibular schwannoma in neurofibromatosis type 2: A retrospective review of 31 patients. *Otol Neurotol* 33(6): 1046–1052.
5. Brieger J, Bedavanija A, Lehr HA, Maurer J, Mann WJ (2003) Expression of angiogenic growth factors in acoustic neurinoma. *Acta Otolaryngol* 123(9):1040–1045.
6. Cayé-Thomasen P, Baandrup L, Jacobsen GK, Thomsen J, Stangerup SE (2003) Immunohistochemical demonstration of vascular endothelial growth factor in vestibular schwannomas correlates to tumor growth rate. *Laryngoscope* 113(12):2129–2134.
7. Plotkin SR, et al. (2009) Hearing improvement after bevacizumab in patients with neurofibromatosis type 2. *N Engl J Med* 361(4):358–367.
8. Blakeley J, et al. (2014) Clinical response to bevacizumab in schwannomatosis. *Neurology* 83(21):1986–1987.
9. Jain RK (2014) Antiangiogenesis strategies revisited: From starving tumors to alleviating hypoxia. *Cancer Cell* 26(5):605–622.
10. Kamoun WS, et al. (2009) Edema control by cediranib, a vascular endothelial growth factor receptor-targeted kinase inhibitor, prolongs survival despite persistent brain tumor growth in mice. *J Clin Oncol* 27(15):2542–2552.
11. Batchelor TT, et al. (2007) AZD2171, a pan-VEGF receptor tyrosine kinase inhibitor, normalizes tumor vasculature and alleviates edema in glioblastoma patients. *Cancer Cell* 11(1):83–95.
12. Yuan F, et al. (1996) Time-dependent vascular regression and permeability changes in established human tumor xenografts induced by an anti-vascular endothelial growth factor/vascular permeability factor antibody. *Proc Natl Acad Sci USA* 93(25): 14765–14770.
13. Kohn RR (1965) Denervation muscle atrophy: An autolytic system in vitro. *Am J Pathol* 47:315–323.
14. Araujo Ap, Araujo M, Swoboda KJ (2009) Vascular perfusion abnormalities in infants with spinal muscular atrophy. *J Pediatr* 155(2):292–294.
15. Lambrechts D, Carmeliet P (2006) VEGF at the neurovascular interface: Therapeutic implications for motor neuron disease. *Biochim Biophys Acta* 1762(11-12):1109–1121.
16. Webber C, Zochodne D (2010) The nerve regenerative microenvironment: Early behavior and partnership of axons and Schwann cells. *Exp Neurol* 223(1):51–59.
17. Höke A (2006) Neuroprotection in the peripheral nervous system: Rationale for more effective therapies. *Arch Neurol* 63(12):1681–1685.
18. Liu J, et al. (2012) TGF-β blockade improves the distribution and efficacy of therapeutics in breast carcinoma by normalizing the tumor stroma. *Proc Natl Acad Sci USA* 109(41):16618–16623.
19. Goel S, et al. (2011) Normalization of the vasculature for treatment of cancer and other diseases. *Physiol Rev* 91(3):1071–1121.
20. Hall EJ (2000) The oxygen effect and reoxygenation. *In Radiobiology for the Radiologist* (JB Lippincott, Philadelphia), pp 91–111.
21. Masuda A, Fisher LM, Oppenheimer ML, Iqbal Z, Slattery WH (2004) Hearing changes after diagnosis in neurofibromatosis type 2. *Otol Neurotol* 25(2):150–154.
22. Parry DM, et al. (1994) Neurofibromatosis 2 (NF2): Clinical characteristics of 63 affected individuals and clinical evidence for heterogeneity. *Am J Med Genet* 52(4): 450–461.
23. Cavanagh JB (1968) Effects of x-irradiation on the proliferation of cells in peripheral nerve during Wallerian degeneration in the rat. *Br J Radiol* 41(484):275–281.
24. Delanian S, Lefaix JL, Pradat PF (2012) Radiation-induced neuropathy in cancer survivors. *Radiother Oncol* 105(3):273–282.
25. Gutmann DH, Giovannini M (2002) Mouse models of neurofibromatosis 1 and 2. *Neoplasia* 4(4):279–290.
26. Giovannini M, et al. (2000) Conditional biallelic Nf2 mutation in the mouse promotes manifestations of human neurofibromatosis type 2. *Genes Dev* 14(13):1617–1630.
27. Wong HK, et al. (2010) Anti-vascular endothelial growth factor therapies as a novel therapeutic approach to treating neurofibromatosis-related tumors. *Cancer Res* 70(9): 3483–3493.
28. Gehlhausen JR, et al. (2015) A murine model of neurofibromatosis type 2 that accurately phenocopies human schwannoma formation. *Hum Mol Genet* 24(1):1–8.
29. Zhang ZG, et al. (2000) VEGF enhances angiogenesis and promotes blood-brain barrier leakage in the ischemic brain. *J Clin Invest* 106(7):829–838.
30. van Bruggen N, et al. (1999) VEGF antagonism reduces edema formation and tissue damage after ischemia/reperfusion injury in the mouse brain. *J Clin Invest* 104(11): 1613–1620.
31. Jin KL, Mao XO, Greenberg DA (2000) Vascular endothelial growth factor: Direct neuroprotective effect in in vitro ischemia. *Proc Natl Acad Sci USA* 97(18): 10242–10247.
32. Jin K, et al. (2001) Caspase-3 and the regulation of hypoxic neuronal death by vascular endothelial growth factor. *Neuroscience* 108(2):351–358.
33. Palmer TD, Willhoite AR, Gage FH (2000) Vascular niche for adult hippocampal neurogenesis. *J Comp Neurol* 425(4):479–494.
34. Lambrechts D, et al. (2003) VEGF is a modifier of amyotrophic lateral sclerosis in mice and humans and protects motoneurons against ischemic death. *Nat Genet* 34(4): 383–394.
35. Carmeliet P, Jain RK (2011) Molecular mechanisms and clinical applications of angiogenesis. *Nature* 473(7347):298–307.
36. Winkler F, et al. (2004) Kinetics of vascular normalization by VEGFR2 blockade governs brain tumor response to radiation: Role of oxygenation, angiopoietin-1, and matrix metalloproteinases. *Cancer Cell* 6(6):553–563.
37. Hurwitz H, et al. (2004) Bevacizumab plus irinotecan, fluorouracil, and leucovorin for metastatic colorectal cancer. *N Engl J Med* 350(23):2335–2342.
38. Landry JC, et al. (2013) Phase 2 study of preoperative radiation with concurrent capecitabine, oxaliplatin, and bevacizumab followed by surgery and postoperative 5-fluorouracil, leucovorin, oxaliplatin (FOLFOX), and bevacizumab in patients with locally advanced rectal cancer: ECOG 3204. *Cancer* 119(8):1521–1527.
39. Kennecke H, et al. (2012) Pre-operative bevacizumab, capecitabine, oxaliplatin and radiation among patients with locally advanced or low rectal cancer: A phase II trial. *Eur J Cancer* 48(1):37–45.
40. Willett CG, et al. (2010) A safety and survival analysis of neoadjuvant bevacizumab with standard chemoradiation in a phase I/II study compared with standard chemoradiation in locally advanced rectal cancer. *Oncologist* 15(8):845–851.
41. Czito BG, et al. (2007) Bevacizumab, oxaliplatin, and capecitabine with radiation therapy in rectal cancer: Phase I trial results. *Int J Radiat Oncol Biol Phys* 68(2): 472–478.
42. Crane CH, et al. (2010) Phase II trial of neoadjuvant bevacizumab, capecitabine, and radiotherapy for locally advanced rectal cancer. *Int J Radiat Oncol Biol Phys* 76(3): 824–830.
43. Nogué M, et al.; AVACROSS Study Group (2011) Addition of bevacizumab to XELOX induction therapy plus concomitant capecitabine-based chemoradiotherapy in magnetic resonance imaging-defined poor-prognosis locally advanced rectal cancer: the AVACROSS study. *Oncologist* 16(5):614–620.
44. Resch G, et al.; Austrian Breast and Colorectal Cancer Study Group (2012) Preoperative treatment with capecitabine, bevacizumab and radiotherapy for primary locally advanced rectal cancer–a two stage phase II clinical trial. *Radiother Oncol* 102(1):10–13.
45. Spigel DR, et al. (2012) Phase II study of bevacizumab and chemoradiation in the preoperative or adjuvant treatment of patients with stage II/III rectal cancer. *Clin Colorectal Cancer* 11(1):45–52.
46. Willett CG, et al. (2005) Surrogate markers for antiangiogenic therapy and dose-limiting toxicities for bevacizumab with radiation and chemotherapy: Continued experience of a phase I trial in rectal cancer patients. *J Clin Oncol* 23(31):8136–8139.
47. Lee JK, Sobel RA, Chiocca EA, Kim TS, Martuza RL (1992) Growth of human acoustic neuromas, neurofibromas and schwannomas in the subrenal capsule and sciatic nerve of the nude mouse. *J Neurooncol* 14(2):101–112.
48. Xu L, et al. (2006) Placenta growth factor overexpression inhibits tumor growth, angiogenesis, and metastasis by depleting vascular endothelial growth factor homodimers in orthotopic mouse models. *Cancer Res* 66(8):3971–3977.
49. Vakoc BJ, et al. (2009) Three-dimensional microscopy of the tumor microenvironment in vivo using optical frequency domain imaging. *Nat Med* 15(10):1219–1223.
50. Sharma N, et al. (2005) Impaired motor learning in mice expressing torsinA with the DYT1 dystonia mutation. *J Neurosci* 25(22):5351–5355.
51. Kamoun WS, et al. (2010) Simultaneous measurement of RBC velocity, flux, hematocrit and shear rate in vascular networks. *Nat Methods* 7(8):655–660.
52. Xu L, Tong R, Cochran DM, Jain RK (2005) Blocking platelet-derived growth factor-D/platelet-derived growth factor receptor beta signaling inhibits human renal cell carcinoma progression in an orthotopic mouse model. *Cancer Res* 65(13):5711–5719.
53. Franken NA, Rodermond HM, Stap J, Haveman J, van Bree C (2006) Clonogenic assay of cells in vitro. *Nat Protoc* 1(5):2315–2319.
54. Xu L, Fidler IJ (2000) Interleukin 8: An autocrine growth factor for human ovarian cancer. *Oncol Res* 12(2):97–106.